CHAPTER V
EXPERIMENTAL RESULTS AND DISCUSSION

5.1 The current-voltage (I-V) characteristics of Heterojunction Bipolar Transistors (HBTs)

After finishing all of HBTs fabrication processes, we determined the basic DC parameters of HBTs with their current-voltage (I-V) characteristics recorded by the curve tracer. The aim of this measurement is not only to examine the DC characteristics of various HBTs but also to distinguish the devices behaviors. Figure 5.1 shows the curve tracer and the probe station for measuring the current –voltage (I-V) characteristics of HBTs.

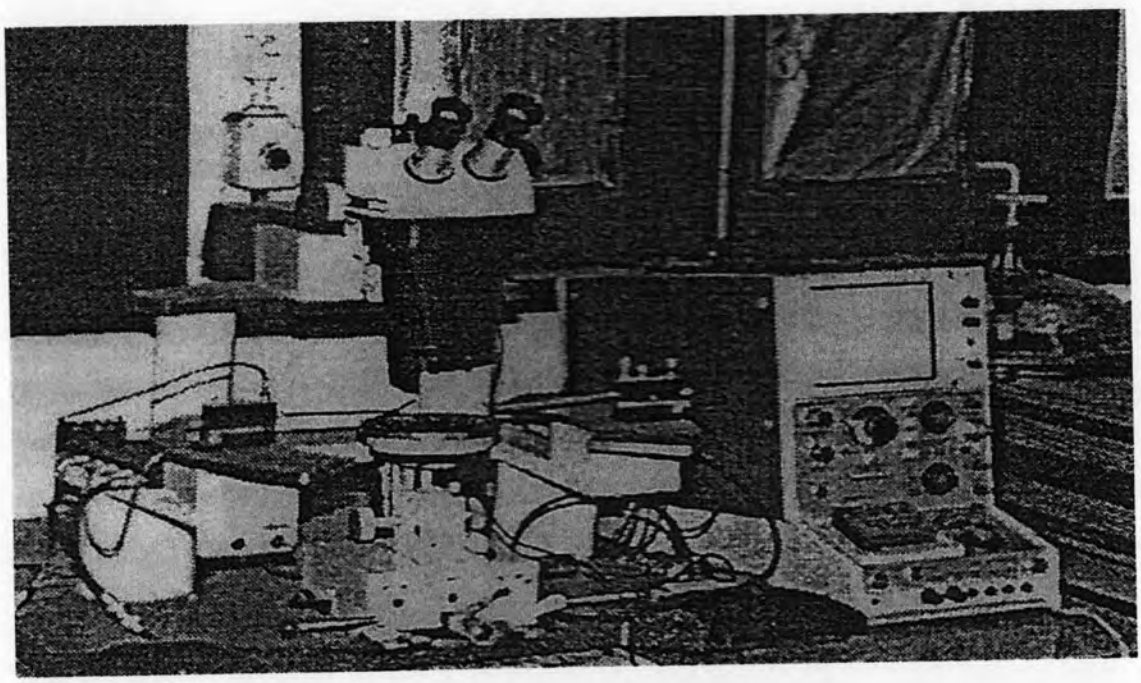

Fig. 5.1 Curve tracer and probe station for measuring the current-voltage characteristics of HBTs

The current voltage characteristics both in normal mode and inverted mode of sample SYMT-04, 07, 08, 10, and 12 are shown in figures 5.2, 5.3, 5.4, 5.5, 5.6, 5.7, 5.8 and 5.9, respectively. Most of HBTs of samples (SYMT-04, 07, 08 and 12) exhibited asymmetric characteristics between both modes except of sample with double regrown base (SYMT-10). Figure 5.2-b is the enlarged normal mode of a HBT of sample SYMT-04, called ST-41 whereas Fig. 5.3-b is the enlarged inverted mode of another HBT of sample SYMT-04 called ST-42. All normal mode characteristics were essentially parallel with the voltage axis, resulting in very high values for the early voltage, meanwhile, some inverted modes had knee-shape characteristic, as clearly seen in Fig. 5.2-c. The offset voltage of most transistors varied in between 60-600 mV that can be seen in table 5.6 and current gains of different transistors with their offset voltages are summarized in tables 5.1, 5.2, 5.3, 5.4 and 5.5.

The graphs of output currents (collector for normal mode, emitter for inverted mode) versus input base currents of different transistors are drawn to express for the symmetry or asymmetry characteristics of the heterojunction bipolar transistors as given in figures 5.10 to 5.20. Moreover, the measured values of input and output currents of every transistor are also shown in tables 5.7 to 5.17.

Current -Voltage (I-V) characteristics curves of GaAs (p^+) regrown base SYMT-04 HBTs

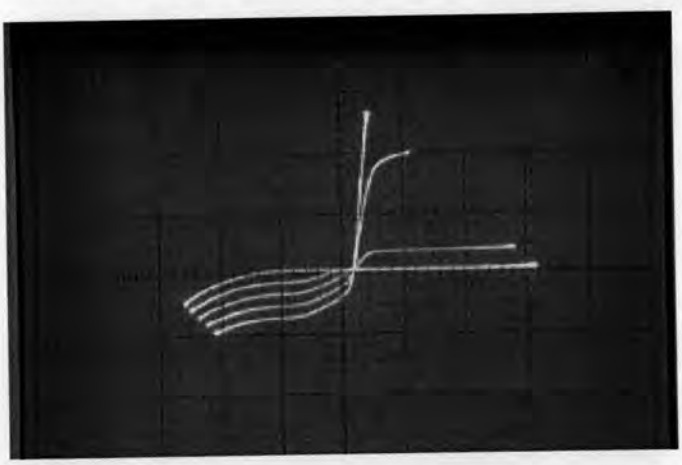

Fig. 5.2-a I-V characteristic of ST-41: I_C (I_E) =2mA/div, V_{CE}=1volt/div, I_B=50μA/step

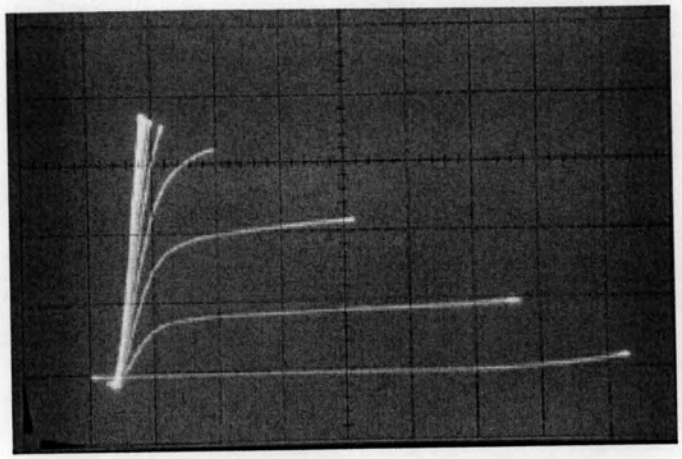

Fig. 5.2-b Enlarge normal mode I-V curve of ST-41: I_C=2mA/div, V_{CE}=0.5V/div, I_B=50μA/step

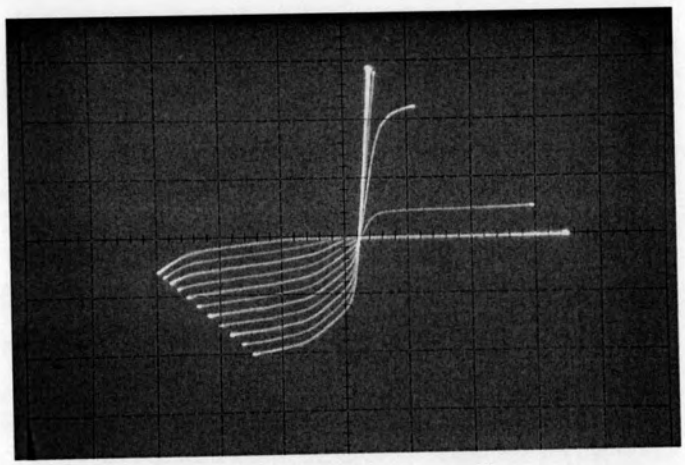

Fig. 5.2-c I-V curve with the knee-shape characteristics of DHBT ST- 43 of SYMT-04: I_C=2mA/div, V_{CE}= 1V/div, I_B=100μA/step

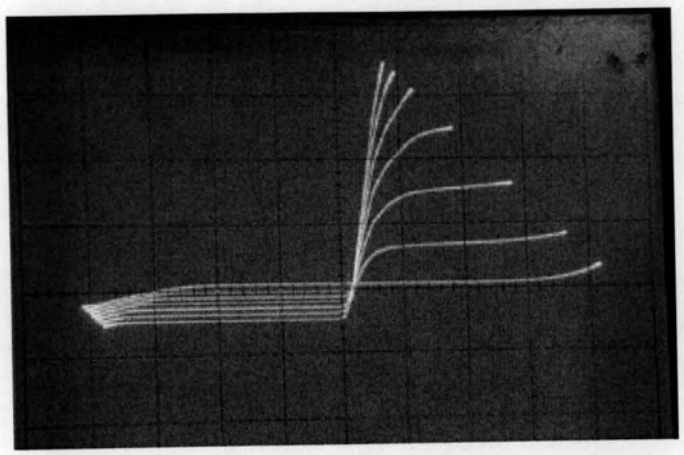

Fig. 5.3-a I-V characteristic of ST-42: I_C (I_E) =2mA/div, V_{CE}=1volt/div, I_B=50μA/step

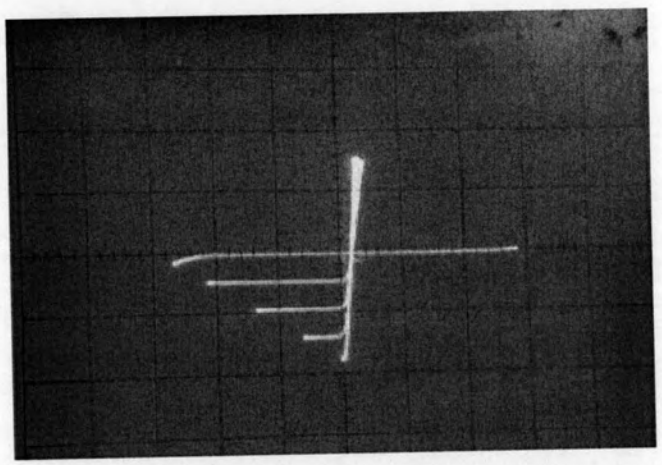

Fig. 5.3-b Enlarge inverted mode of ST-42 I-V curve: I_E=1mA/div, V_{CE}=1V/div, I_B=100μA/step

Current -Voltage (I-V) characteristics curves of P^+-$Ga_{0.8}Al_{0.2}As$ regrown base HBTs with N- $Ga_{0.8}Al_{0.2}As$ Collector (SYMT-07)

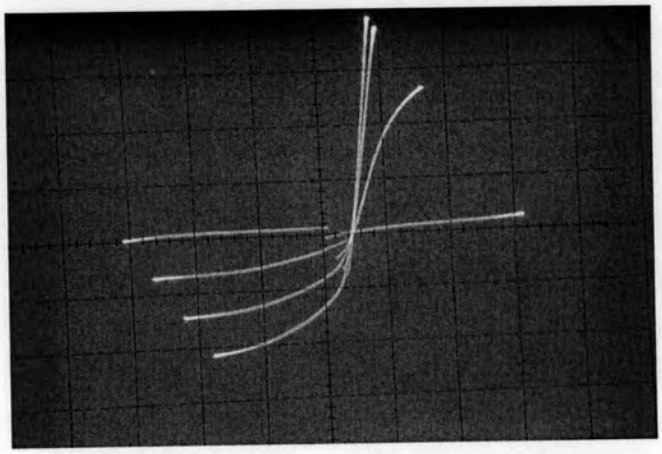

Fig. 5.4 I-V characteristic of ST-71: I_C (I_E) = 2mA/div,V_{CE}=0.5volt/div, I_B=0.2mA/step

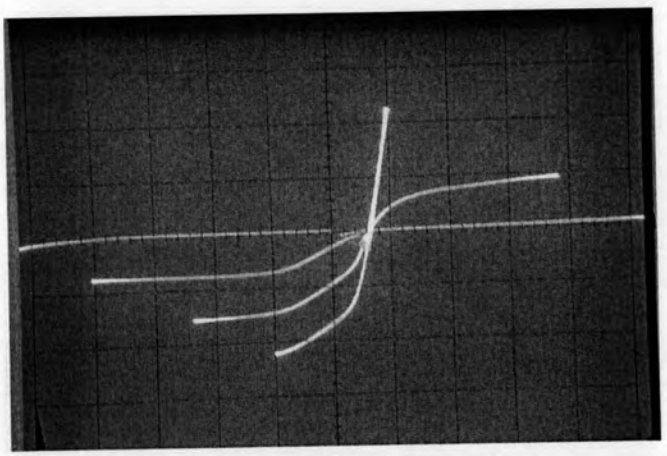

Fig. 5.5 I-V characteristic of ST-72: I_C (I_E) =2mA/div, V_{CE}=0.5volt/div, I_B=0.2mA/step

Current -Voltage (I-V) characteristics curve of P^+-$Ga_{0.8}Al_{0.2}As$ regrown base HBTs with N- $Ga_{0.7}Al_{0.3}As$ Collector (SYMT-08)

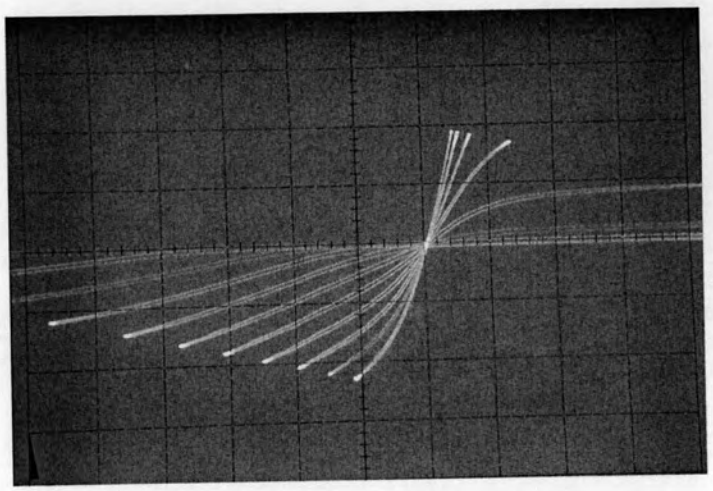

Fig. 5.6 I-V characteristic of ST-81: I_C (I_E) =1mA/div, V_{CE}=0.1volt/div, I_B=0.1mA/step

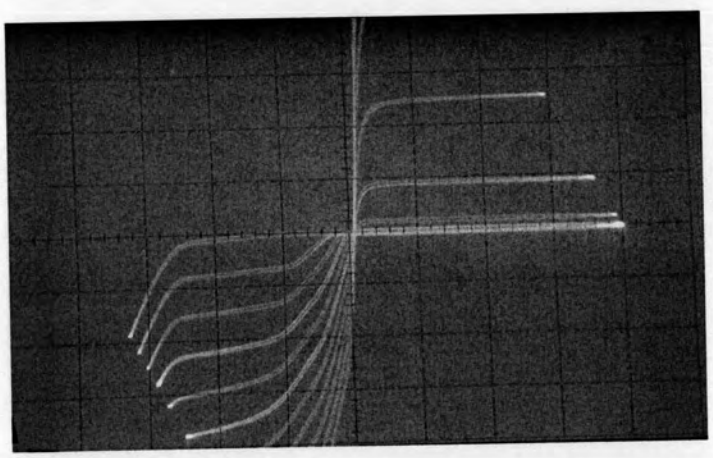

Fig.5.7 I-V characteristic of ST-82: I_C (I_E) =1mA/div, V_{CE}=1volt/div,I_B=0.1mA/step

Current -Voltage (I-V) characteristics curve of double regrown base HBTs (SYMT-10)

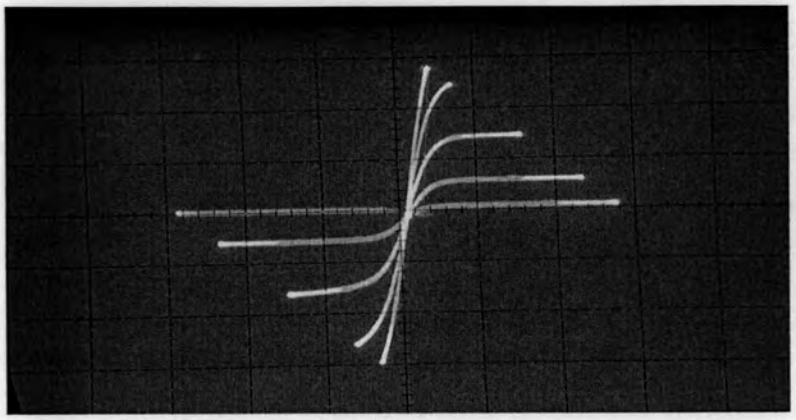

Fig. 5.8-a I-V characteristic of ST-101 with offset voltage of 60mV: I_C (I_E) =1mA/div, V_{CE}=0.5volt/div, I_B=50μA/step

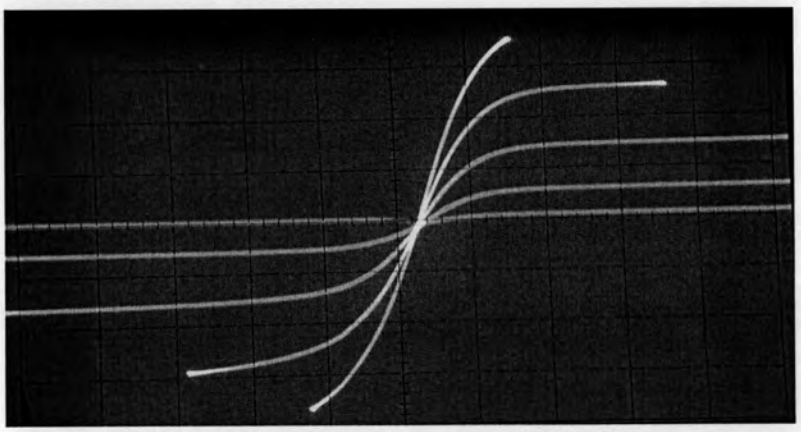

Fig. 5.8-b I-V characteristic of ST-101 with offset voltage of 60mV: I_C (I_E) =1mA/div, V_{CE}=0.2volt/div, I_B=50μA/step

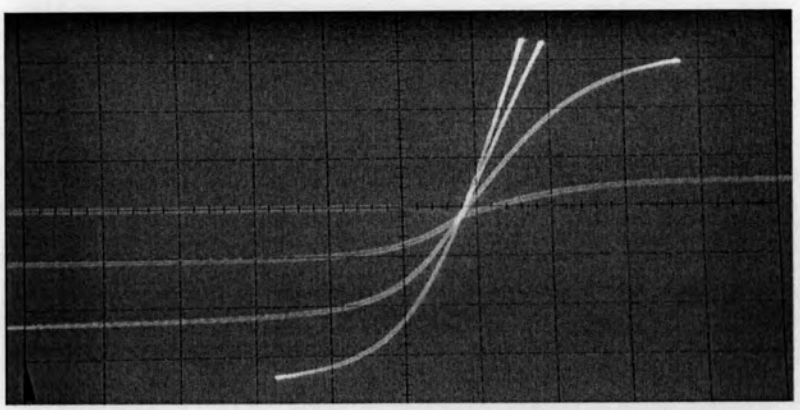

Fig. 5.8-c I-V characteristic of ST-102 with offset voltage of 80mV: I_C (I_E) =1mA/div, V_{CE}=0.1volt/div, I_B=0.1mA/step

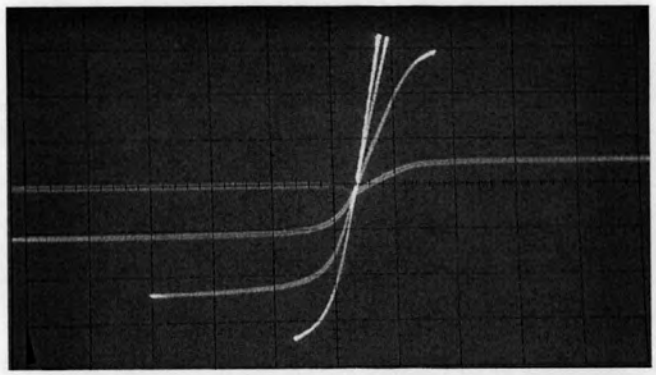

Fig. 5.8-d I-V characteristic of ST-102 with offset voltage of 80mV: I_C (I_E) =1mA/div, V_{CE}=0.2volt/div, I_B=0.1mA/step

Current -Voltage (I-V) characteristics curve of diffuse base HBTs (SYMT-12)

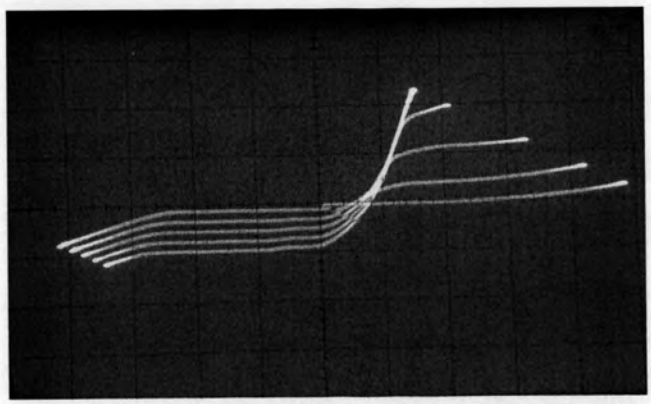

Fig. 5.9-a I-V characteristic of ST-121: I_C (I_E) =1mA/div, V_{CE}=1volt/div I_B=20μA/step

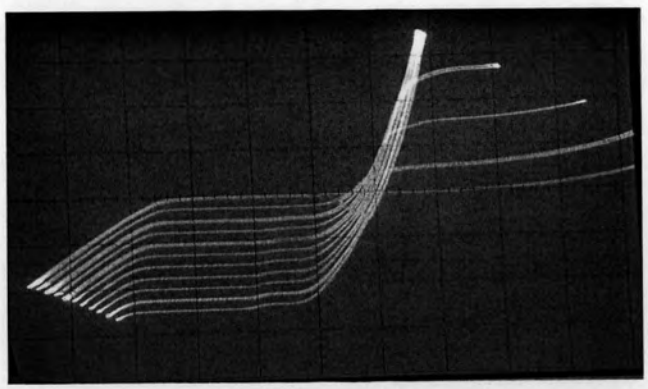

Fig.5.9-b I-V characteristic of ST-123: I_C (I_E) =1mA/div, V_{CE}=1volt/div, I_B = 50 μ A/step

Transistors(HBT)	Normal mode Gain at (I_C,V_{CE})	Inverted mode Gain at (I_E,V_{CE})	V_{CE} Offset voltages (V)
ST-41	40 (2mA,1V)	8 (1mA,1V)	0.2
ST-42	30 (5mA,2V)	5 (1mA,2V)	0.2
ST-43	20 (4mA,1V)	4 (4mA,1V)	0.2

Table 5.1 Current gains of HBTs and V_{CE} offset voltages of different SYMT-04 samples

Transistors(HBT)	Normal mode Gain at (I_C,V_{CE})	Inverted mode Gain at (I_E,V_{CE})	V_{CE} Offset voltages (V)
ST-71	30 (6mA,0.5V)	8 (1.6mA,0.5V)	0.25
ST-72	10 (2mA,0.5V)	7 (1.4mA,0.5V)	0.3

Table 5.2 Current gains of HBTs and V_{CE} offset voltages of different SYMT-07 samples

Transistors(HBT)	Normal mode Gain at (I_C,V_{CE})	Inverted mode Gain at (I_E,V_{CE})	V_{CE} Offset voltages (V)
ST-81	10 (3mA,0.1V)	5 (1.5mA,0.1V)	0.1
ST-82	8.33 (2.5mA,1V)	6.66 (2mA,1V)	0.1

Table 5.3 Current gains of HBTs and V_{CE} offset voltages of different SYMT-08 samples

Transistors(HBT)	Normal mode Gain at (I_C,V_{CE})	Inverted mode Gain at (I_E,V_{CE})	V_{CE} Offset voltages (mV)
ST-101	15 (1.5mA,0.5V)	16 (1.6mA,0.5V)	60
ST-101	17.33 (2.6mA,0.2V)	18 (2.7mA,0.2V)	60
ST-102	13.33 (3.8mA,0.1V)	7.33 (2.2mA,0.1V)	80
ST-102	14 (4.2mA,0.2V)	8 (2.4mA,0.2V)	80

Table 5.4 Current gains of HBTs and V_{CE} offset voltages of SYMT-10 samples

Transistors(HBT)	Normal mode Gain at (I_C,V_{CE})	Inverted mode Gain at (I_E,V_{CE})	V_{CE} Offset voltages (V)
ST-121	41.66 (2.5mA,1V)	13.33 (0.8mA,1V)	0.6
ST-122	18 (1.8mA,1V)	5 (0.5mA,1V)	0.6

Table 5.5 Current gains of HBTs and V_{CE} offset voltages of different SYMT-12 samples

Transistor	Sample-Name	Offset Voltage
p^+-GaAs Single Regrown Base	SYMT-04	200mV
P^+-$Ga_{0.8}Al_{0.2}As$ Single Regrown Base	SYMT-07	250mV
P^+-$Ga_{0.8}Al_{0.3}As$ Single Regrown Base	SYMT-08	100mV
p^+-GaAs/ P^+-$Ga_{0.8}Al_{0.2}As$ Double Regrown Base	SYMT-10	60mV
Diffuse Base	SYMT-12	600mV

Table 5.6 V_{CE} offset voltages of different transistors

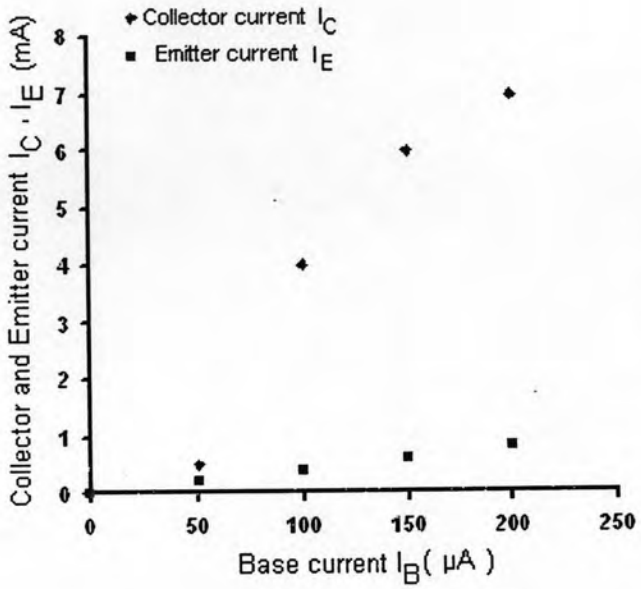

Input Base Current I_B(μA)	Output Collector Current I_C(mA)	Output Emitter Current I_E(mA)
0	0	0
50	0.5	0.2
100	4	0.4
150	6	0.6
200	7	0.8

Fig. 5.10 Graph of output collector and output emitter current versus input base current of ST-41 DHBT

Table 5.7 Right: Measured current values of ST-41 DHBT

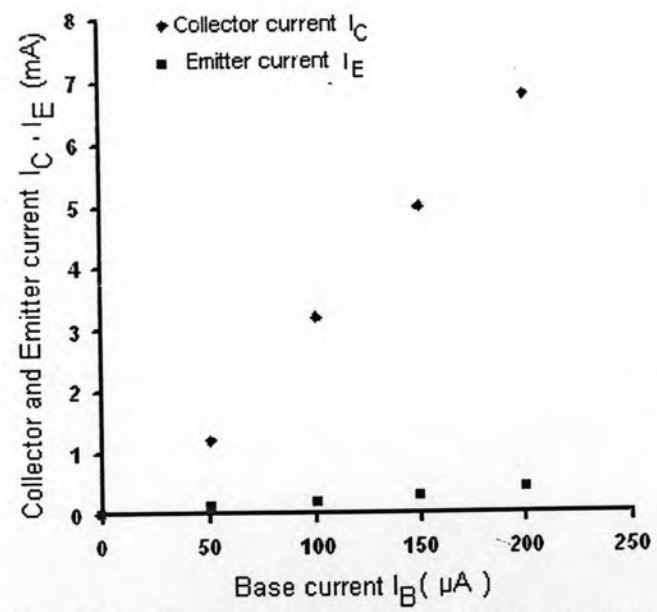

Input Base Current I_B(μA)	Output Collector Current I_C(mA)	Output Emitter Current I_E(mA)
0	0	
50	1.2	0.1
100	3.2	0.2
150	5	0.3
200	6.8	0.4
250	8	0.5

Fig. 5.11 Graph of output collector and output emitter current versus input base current of ST-42 DHBT

Table 5.8 Right: Measured current values of ST-42 DHBT

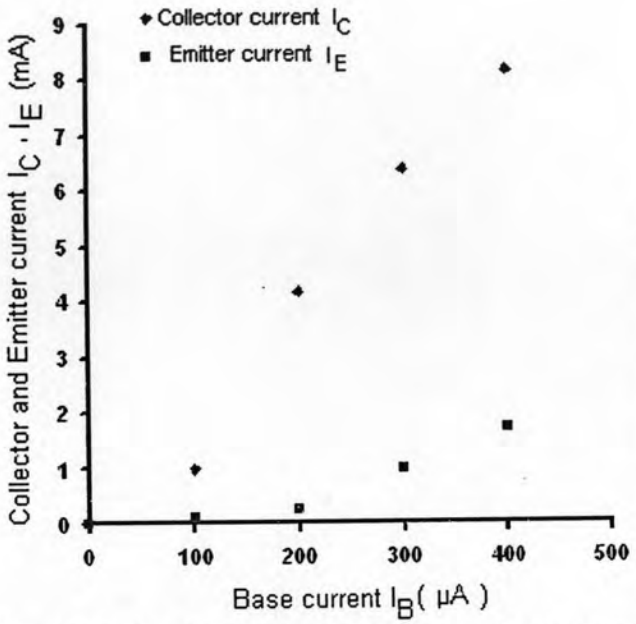

Input Base current I_B(μA)	Output Collector current I_C(mA)	Output Emitter current I_E(mA)
0	0	0
100	1	0.1
200	4.2	0.25
300	6.4	1
400	8.2	1.7

Fig. 5.12 Graph of output collector and output emitter current versus input base current of ST-43 DHBT

Table 5.9 Right: Measured current values of ST-43 DHBT

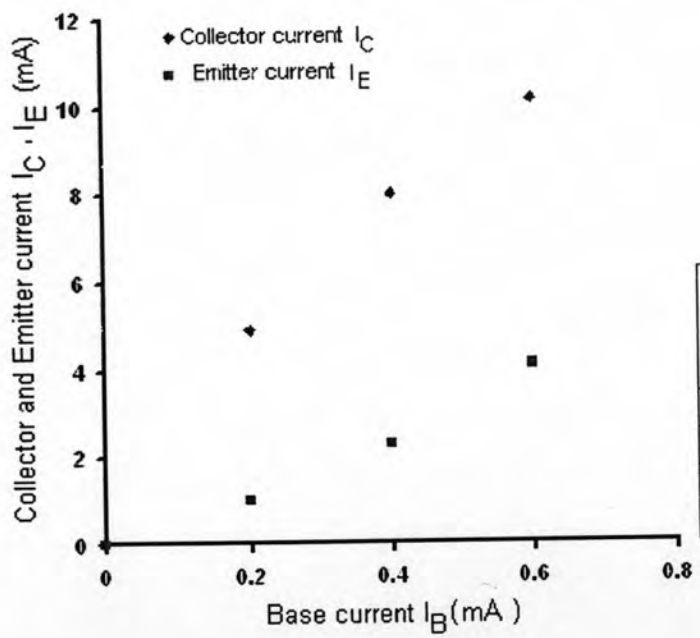

Input Base current I_B(mA)	Output Collector current I_C(mA)	Output Emitter current I_E(mA)
0	0	0
0.2	4.9	1
0.4	8	2.3
0.6	10.2	4.1

Fig. 5.13 Graph of output collector and output emitter current versus input base current of ST-71 DHBT

Table 5.10 Right: Measured current values of ST-71 DHBT

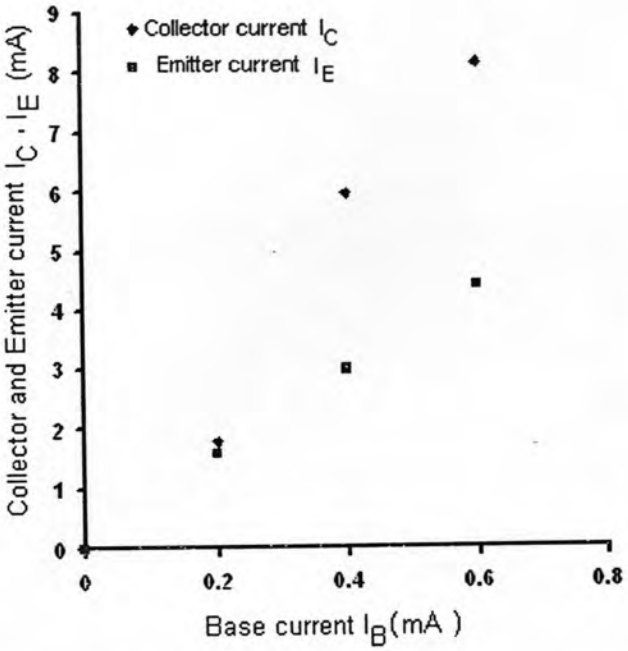

Input Base current I_B(mA)	Output Collector current I_C(mA)	Output Emitter current I_E(mA)
0	0	0
0.2	1.8	1.6
0.4	6	3
0.6	8.2	4.4

Fig. 5.14 Graph of output collector and output emitter current versus input base current of ST-72 DHBT

Table 5.11 Right: Measured current values of ST-72 DHBT

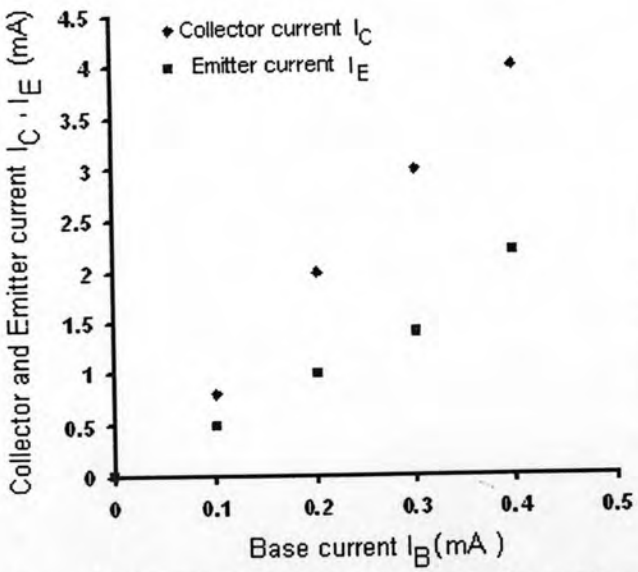

Input Base current I_B(mA)	Output Collector current I_C(mA)	Output Emitter current I_E(mA)
0	0	0
0.1	0.8	0.5
0.2	2	1
0.3	3	1.4
0.4	4	2.2

Fig. 5.15 Graph of output collector and output emitter current versus input base current of ST-81 DHBT

Table 5.12 Right: Measured current values of ST-81 DHBT

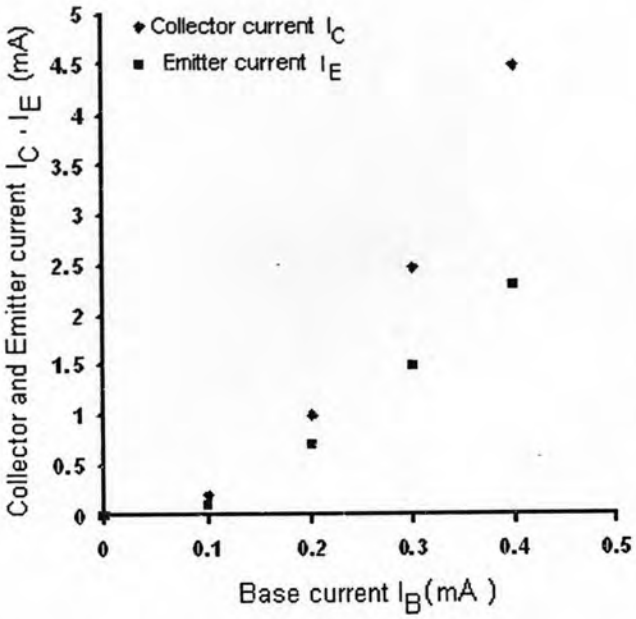

Input Base current I_B(mA)	Output Collector current I_C(mA)	Output Emitter current I_E(mA)
0	0	0
0.1	0.2	0.1
0.2	1	0.7
0.3	2.5	1.5
0.4	4.5	2.3

Fig. 5.16 Graph of output collector and output emitter current versus input base current of ST-82 DHBT

Table 5.13 Right: Measured current values of ST-82 DHBT

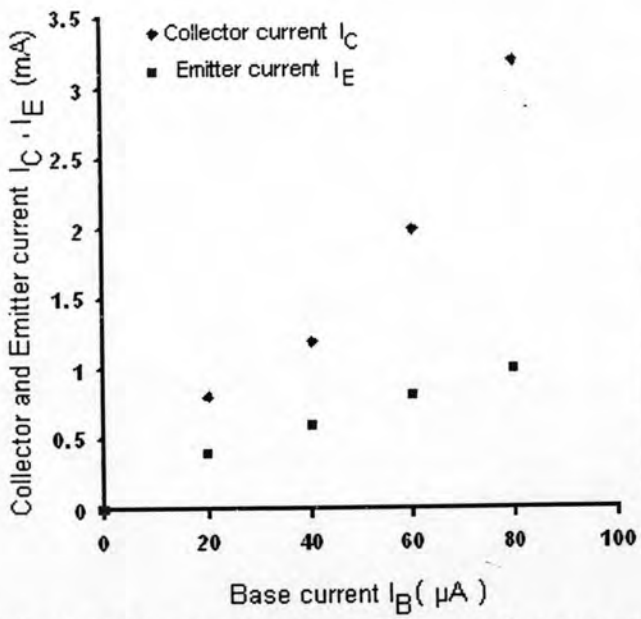

Input Base current I_B(μA)	Output Collector current I_C(mA)	Output Emitter current I_E(mA)
0	0	0
20	0.8	0.4
40	1.2	0.6
60	2	0.8
80	3.2	1

Fig. 5.17 Graph of output collector and output emitter current versus input base current of ST-121 DHBT

Table 5.14 Right: Measured current values of ST-121 DHBT

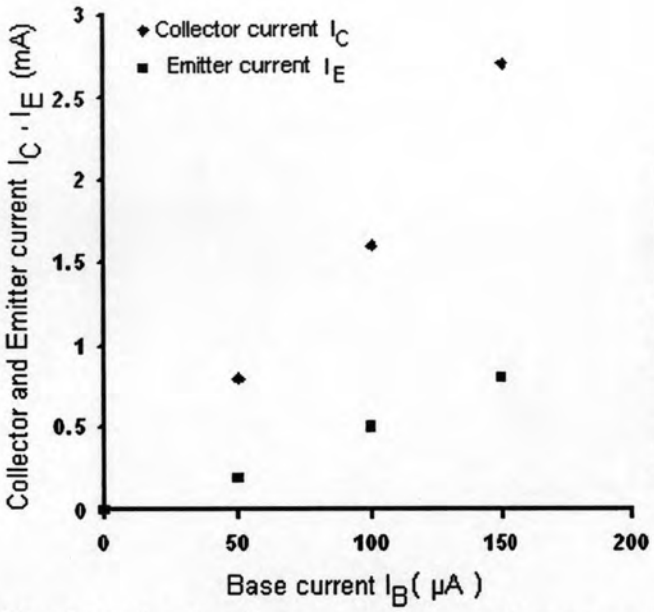

Input Base current I_B(μA)	Output Collector current I_C(mA)	Output Emitter current I_E(mA)
0	0	0
50	0.8	0.2
100	1.6	0.5
150	2.7	0.8
200	3.8	1

Fig. 5.18 Graph of output collector and output emitter current versus input base current of ST-122 DHBT

Table 5.15 Right: Measured current values of ST-122 DHBT

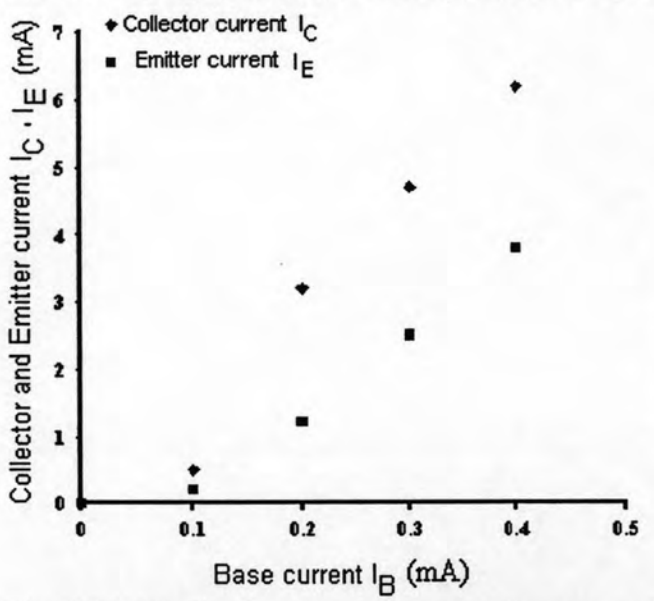

Input Base current I_B(mA)	Output Collector current I_C(mA)	Output Emitter current I_E(mA)
0	0	0
0.1	0.5	0.2
0.2	3.2	1.2
0.3	4.7	2.5
0.4	6.2	3.8

Fig. 5.19 Graph of output collector and output emitter current versus input base current of ST-102 DHBT

Table 5.16 Right: Measured current values of ST-102 DHBT

Input Base current $I_B(\mu A)$	Output Collector current $I_C(mA)$	Output Emitter current $I_E(mA)$
0	0	0
50	0.5	0.6
100	1.5	1.6
150	2.6	2.8
200	3.8	3.8

Table 5.17 Measured current values of ST-101 DHBT

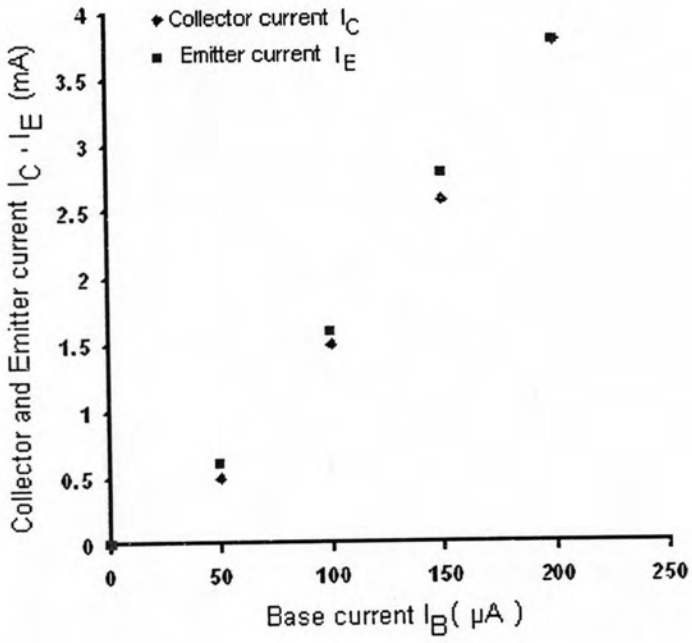

Fig. 5.20 Graph of output collector and output emitter current versus input base current of ST-101 DHBT

5.2 Discussion

The heterojunction bipolar transistors with the single p^+-GaAs regrown base layer showed the asymmetric I-V characteristics as seen in figures 5.2 to 5.3. Especially, the normal mode gains were approximately five to six times higher than that of inverted mode gains for almost transistors even though the same composition of the aluminum contents fixed as 0.2 and same carrier concentration of emitter and collector about $10^{17}cm^{-3}$ were used. The physical structure for all of (DHBTs) is really asymmetric which has the collector-base junction area is larger than the emitter-base junction area, as clearly seen in Fig. 5.21.

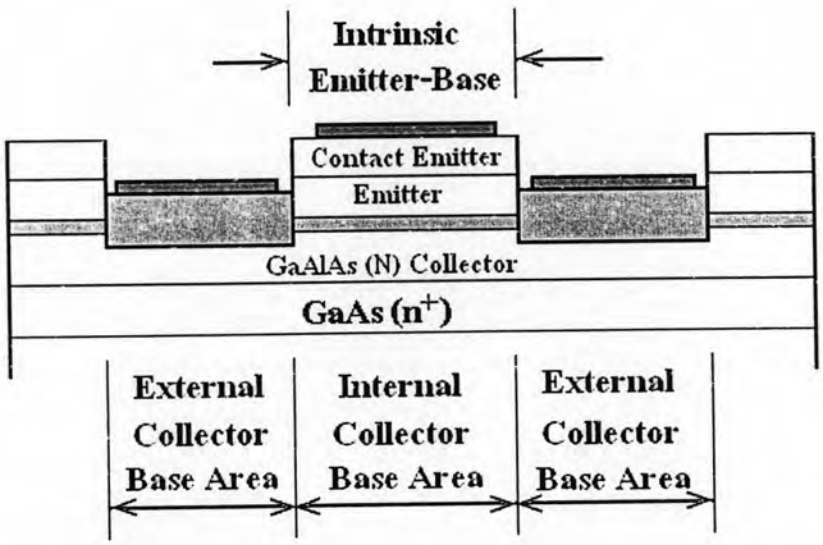

Fig. 5.21 Physical structure of designed transistor (DHBT), showing the external and internal collector base area

As the collector-base junction is the forward biased in the inverted mode, the collector injects the electrons (which is similar to the emitter-base junction under the normal mode condition) in both internal and external base area. Most of electrons injected outside of the internal emitter base junction of the DHBTs are mainly lost by the recombination, resulting in lower current gains in the inverted mode. Moreover, the controlling of the etching depth during fabrication process is very important to define the external base area or regrown base area. The etching depth must be precisely controlled in between N-GaAlAs collector layer and also the top of the external regrown base layer should be in between N-GaAlAs emitter layer as shown schematically in chapter 4, figure 4.25-d.

If the etching depth is far beyond the collector layer down to the n^+-GaAs buffer layer, as shown schematically with cross section diagram in Fig. 5.22. The regrown base layer will perform as p^+ - GaAs / n^+- GaAs homojunction in the external base area of the HBTs parallel to the p^+ - GaAs / N- GaAlAs heterojunction under the internal base area. Since the energy barrier against injected holes of homojunction is lower compared to that of heterojunction as seen in Fig. 5.23. Most of holes can be easily flow from the base to the collector outside internal CB junction area. The base current I_B therefore increases under the inverted mode resulting in lower dc-current gain. These transistors effectively behave as a homojunction bipolar transistor with lower current gains.

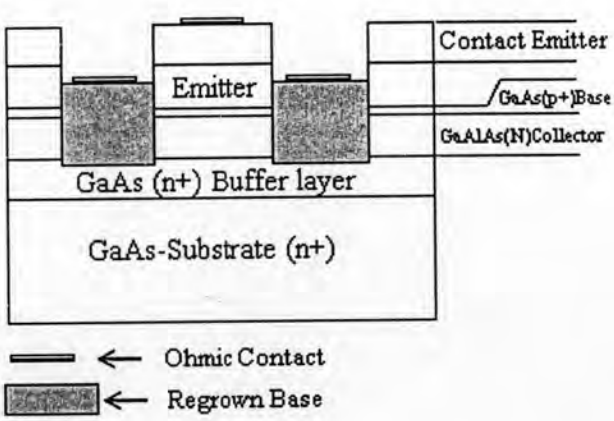

Fig.5.22 Define the regrown base area deep to around the n^+-GaAs Buffer layer

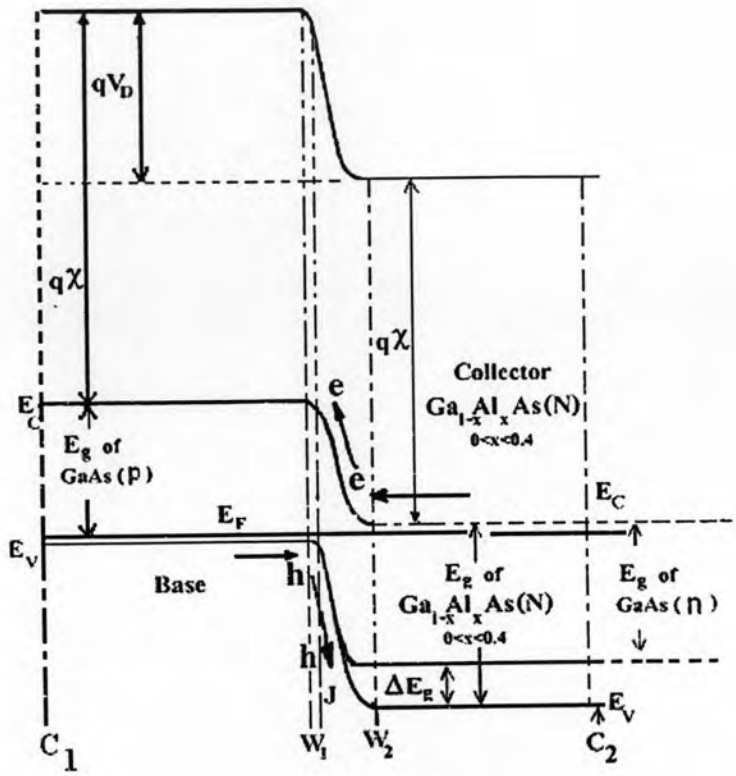

Fig. 5.23 Band diagram of Collector-Base junction with superimposing between the bangap of GaAs (n^+) substrate and GaAlas (N) collector on the right side

If the etching depth for the regrown base area doesn't reach to the base layer as seen in Fig. 5.24, the internal base region of the original structure can't connect to the external base region. So, this kind of transistor can't work.

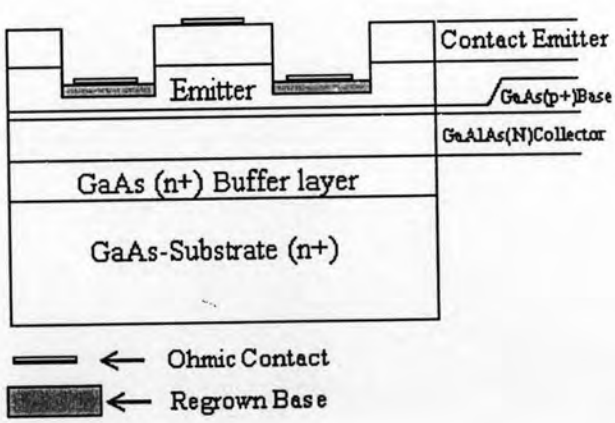

Fig. 5.24 Define the regrown base area just reach to the N-GaAlAs emitter layer

Furthermore, the knee-shape characteristics occurred due to the spike effects at the emitter-base heterojunctions which can be seen clearly in the band diagram of Fig. 5.26. In the band diagram of Fig. 5.26, the electrons can be injected from the collector-base junction with the forward biased under inverted mode but they can not flow easily through the emitter-base heterojunction due to the spikes effect .As the reverse bias voltage at emitter-base junction is more and more, the energy band of emitter moves down with respect to that of the base. The height of spike is then lower resulting in slowly increasing of the output emitter current. The knee-shape characteristics exhibited in most of inverted mode of SYMT-04 as shown in Fig. 5.25.

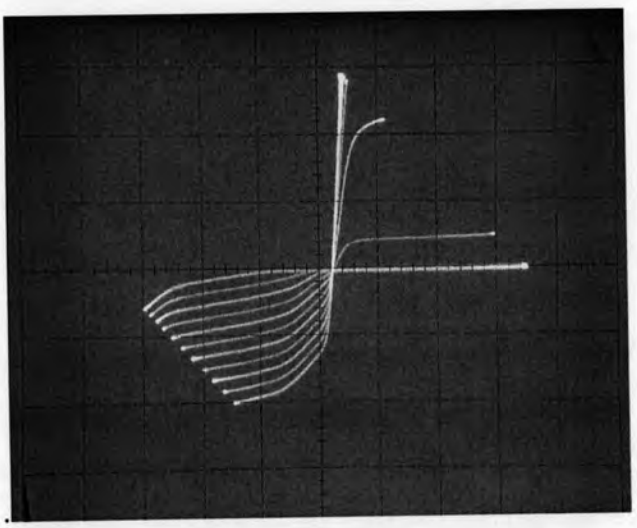

Fig. 5.25 I-V curve with the knee-shape characteristics of DHBT ST-43 of SYMT-04

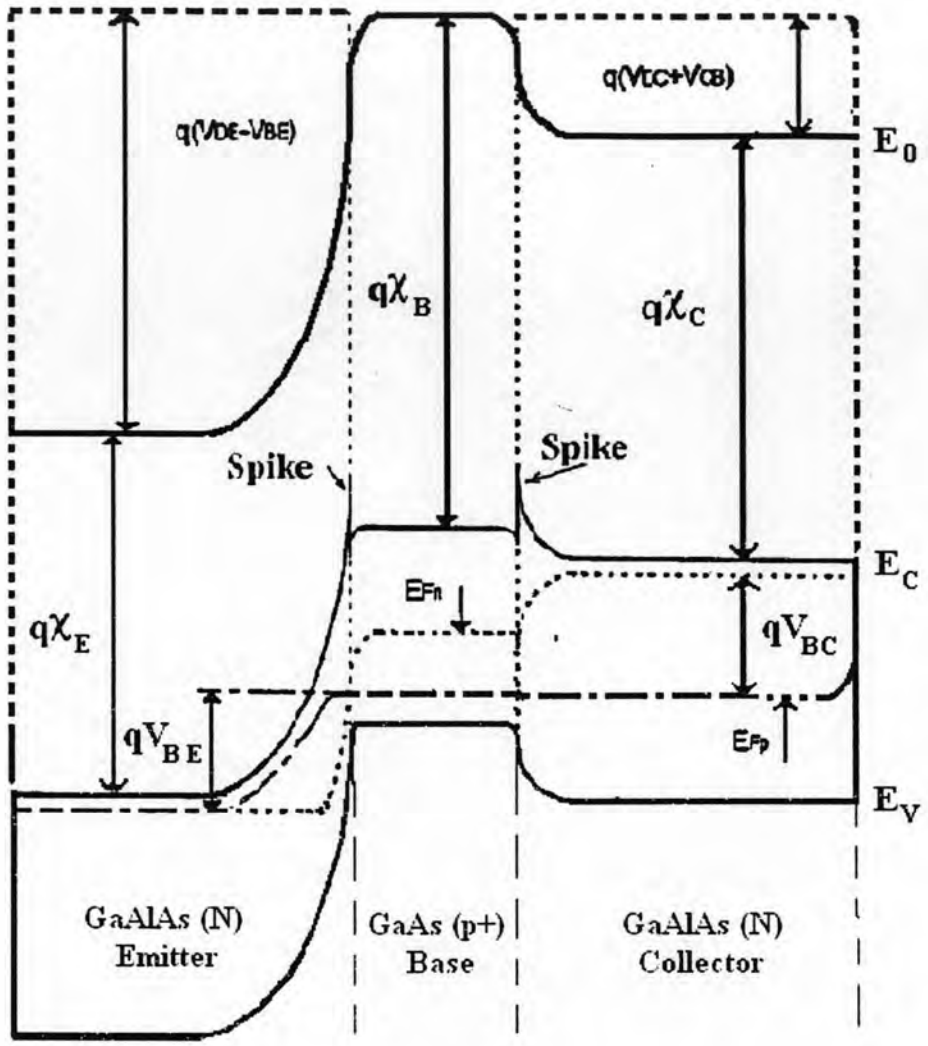

Fig. 5.26 Band diagram of DHBTs

All DHBTs with $Ga_{1-x}Al_xAs$ (x=0.2) external base showed more symmetric with the normal mode gains two to three time greater than that of the inverted mode gains, as shown in figures 5.4 to 5.7. Eventually, single regrown base layer - $Ga_{1-x}Al_xAs$ (x=0.2) from the second growth was used to improve the current gain in the inverted mode. The collector-base junction formed between the external base $Ga_{1-x}Al_xAs$ (x=0.2) and collector-$Ga_{1-x}Al_xAs$ (N) has the barrier of the electron higher than that of intrinsic heterojunction. This high barrier will suppress the injection of electrons from the external collector-base junction, consequently HBT exhibit a higher gains in the inverted mode. The results of samples SYMT-07 and 08 therefore were more symmetric compared to all

samples of SYMT-04. However, there are two side effects for using $Ga_{0.8}Al_{0.2}As$ regrown base. Firstly, more recombination centers in the regrown base region and secondly, worse base ohmic contact. These will degrade the transistor performance.

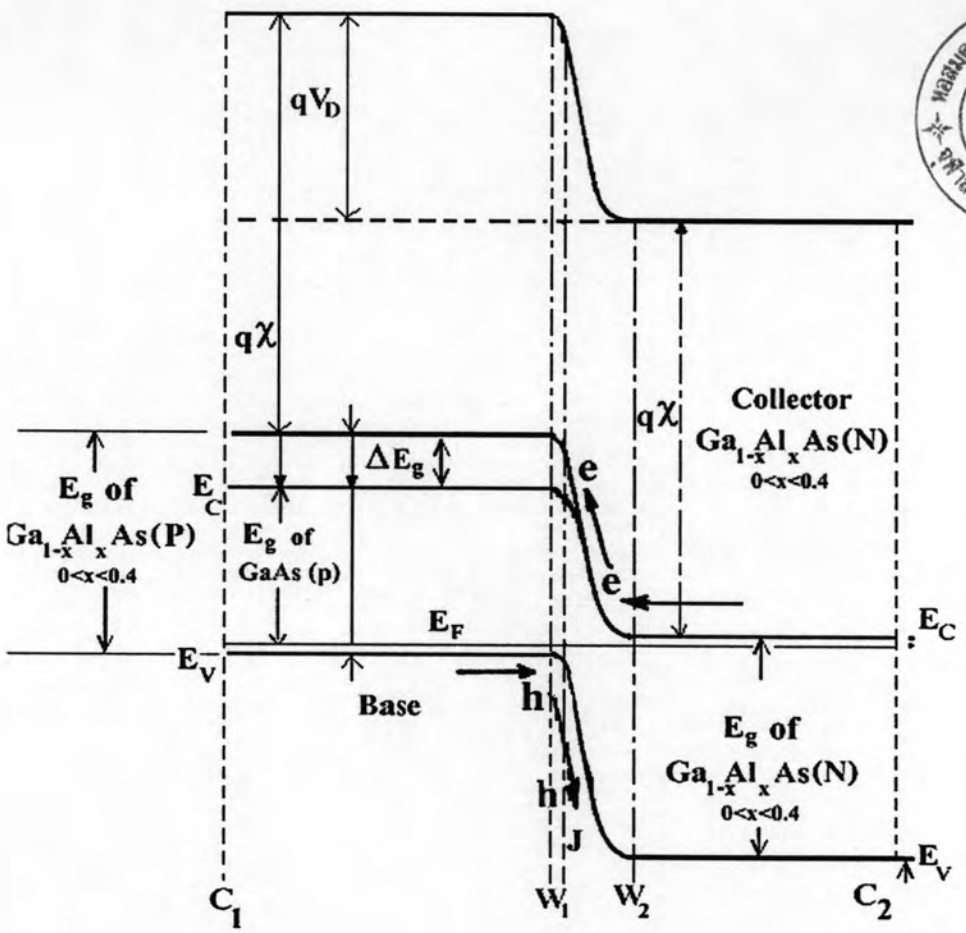

Fig. 5.27 Band diagram of Collector-Base junction in DHBT with superimposing between the bandgap of External Base - $Ga_{1-x}Al_xAs(x=0.2)$ and Ga As on the left side

The heterojunction bipolar transistors with double regrown base layer or double external base layer showed ***the symmetrical I-V characteristics*** as seen in figures 5.8-a, and b. The normal mode gains are almost equal to the inverted mode gains for almost transistors. In other words, the output collector current and output emitter current are almost equivalent while operating in normal and inverted modes with the same input base current steps, as clearly seen in Fig. 5.20.This is because the junction formed by P^+-$Ga_{0.8}Al_{0.2}As$ lower base layer and N- $Ga_{1-x}Al_xAs$ collector layer in the external base region can suppress the injection of electrons in inverted mode, and also the electron recombination in the double regrown base region is lower compared to that in P^+-$Ga_{0.8}Al_{0.2}As$ single regrown base. Moreover the aluminum content in collector is adjusted a little higher to 0.3 to increase in collector injection efficiency. For these reasons, the base current is lower, resulting of higher gain in inverted mode. However, one side effect to the normal mode gain, more aluminum content in collector result to a higher spike at the CB junction due to more difference of energy gap of the collector and the base. These spikes cause the normal mode gain to decrease. The normal mode gain decreases, while the inverted mode gain increases. Both mode gains can go across each other, resulting to the symmetrical point.

The heterojunction bipolar transistors with diffuse base showed asymmetric I-V characteristics with similar fashion as those of single regrown base as seen in figures 5.9-a, b, c. Especially, the normal mode gains were approximately two to three times higher than that of inverted mode gains for almost transistors with a large amount of offset voltage. As mentioned in chapter 2, according to Eq.(2.47), the offset voltage depends on emitter resistance, the ratio between the area of collector-base to emitter-base junction and also the inverted mode gain. But, in practice, the offset voltage can be evaluated by the difference between the (I, V) characteristics of emitter-base and collector-base junctions with the third terminal opened as shown in figures 5.28, 5.29, 5.30. The differences between two I-V curves at a fixed current will be contribute to the amount of offset voltage and the offset voltage does not depend on the base current in ideal cases. But, in some devices with appreciable emitter resistance, the offset voltage was found to be depending on the base current step as clearly seen in Fig. 5.9-b. This result gives evidence of term $I_E R_E$ in the offset voltage equation (2.47). The large emitter resistance is

usually due to the combination of high contact resistance and bulk emitter series resistance and then it seems to be more affected by device parameters rather than the material parameters. Therefore the large offset voltages were found to originate from the large differences between the EB and CB junction voltages as seen figures 5.28-a, b for diffused base and figures 5.29-a, b for single regrown base of GaAs (p^+).

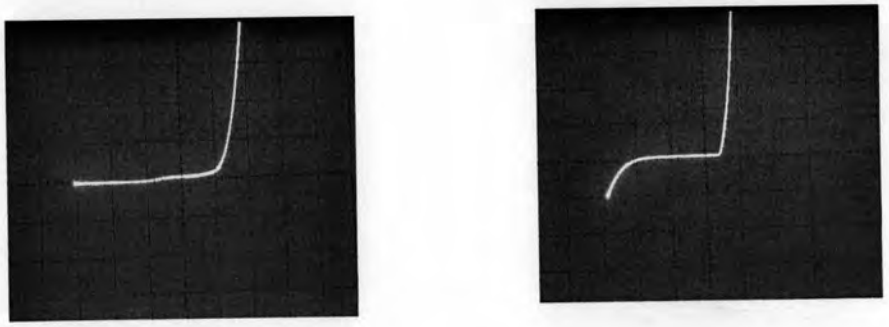

Fig.5.28 (a-Left): Emitter-Base Diode current (b-Right): Collector-Base Diode current for HBTs with diffuse base: Vertical scale I = 1 mA, Horizontal scale V = 2V

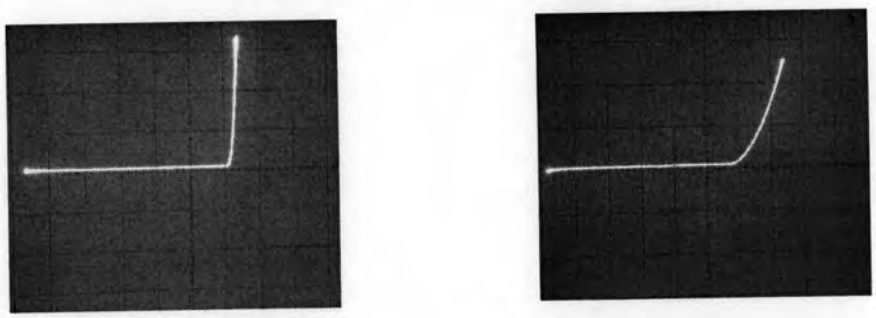

Fig.5.29 (a- Left): Emitter-Base Diode current (b- Right): Collector-Base Diode current for HBTs with single regrown base: Vertical scale I=2mA; Horizontal scale V=1V

In case of GaAs (p^+)/$Ga_{0.8}Al_{0.2}As$ (P^+) double regrown base SYMT-10, the $V_{CE,offset}$ voltage of almost HBTs in sample SYMT-10 was low due to the small difference between the (I-V) of emitter-base junction and collector-base junction as seen in figures 5.30-a, b. This result proves that the second and third terms of offset voltage equation (4.27) have low contribution. In other words, the effective areas of both junctions are nearly equal and also the inverted mode gain is high.

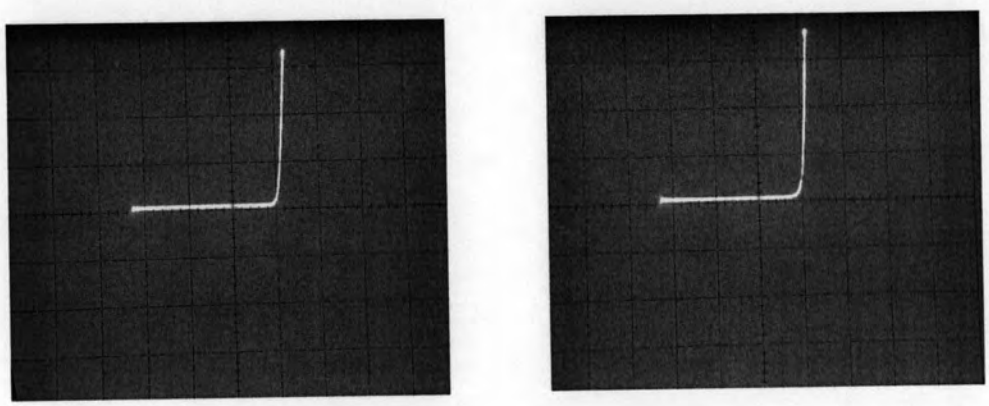

Fig. 5.30 (a- Left) Emitter-Base Diode characteristic (b- Right) Collector- Base Diode characteristic for double regrown base HBTs: Vertical scale I=2mA, Horizontal scale V=1V